Proceedings of the 28th IEEE
EMBS Annual International Conference
New York City, USA, Aug 30-Sept 3, 2006

Reconstruction of Central Aortic Pressure Waveform Using Adaptive Multi-Channel Identification

Jin-Oh Hahn, Andrew Reisner, Horacio Hojman, H. Harry Asada

Abstract— **This paper presents an adaptive multi-channel (AMC) approach for the reconstruction of the central aortic blood pressure (BP) waveform from multiple peripheral BP measurements. In contrast to most of the previously developed single-channel methods for estimating central aortic BP waveform, the key merit of the AMC algorithm is its ability to be individualized without any prior model training or parameter tuning. Preliminary experimental evaluation of the AMC algorithm with respect to a single channel approach in a swine model shows 17.4% improvement in the waveform reconstruction accuracy in terms of RMSE (from 3.3 mmHg for the single-channel approach to 2.8 mmHg for the AMC algorithm) and the superior prediction of several key central aortic BP waveform features (from 0.1512 to 0.9109 for the ejection duration, in terms of r^2 values). These results suggest that the AMC algorithm can render a very accurate reconstruction of the central aortic BP waveform from two peripheral BP measurements without any prior model training or parameter tuning.**

Index Terms— **Central aortic blood pressure reconstruction, adaptive multi-channel identification, asymmetric T-tube model, generalized transfer function, ejection duration.**

I. Introduction

FEATURES of the central aortic pressure waveform, such as its systolic BP, pressure rise time, ejection duration and augmentation index, have been accepted as useful indices of key cardiovascular phenomenon such as afterload, cardiac inotropy, arterial compliance and peripheral resistance. Although physiologically meaningful, direct measurement of the central aortic BP is so invasive that it is rarely used in the clinical care or research.

A more common, less invasive alternative has been the reconstruction of the central aortic BP waveform from a peripheral arterial BP waveform. The identification of the pressure transfer dynamics between the aorta and the peripheral measurement site has been the essential part of this approach [1,2,3,4]. This approach has a major shortcoming: the central aortic BP must be measured together with its peripheral counterpart to characterize the aortic-to-peripheral pressure transfer dynamics. For this reason, most of the previous indirect methods for the reconstruction of the central aortic BP waveform could not be applied on a per-patient basis; instead, a generalized transfer function (GTF) identified from a group of patients for whom the invasive central aortic BP measurement is possible has been used to estimate the central aortic BP of the general population. Although it has been argued that some of the upper-limb pressure transfer dynamics exhibit a reasonable level of consistency and small subject-to-subject and temporal variability in the low- and mid-frequency range [1], the idea of applying the GTF to the general population still suffers from controversy [5,6]. In effect, the discrepancy between the pressure transfer dynamics of individual patients and the GTF is unavoidable, and the brute-force application of the GTF might be susceptible to errors in the reconstruction of the central aortic BP waveform as well as the extraction of the clinical features therein. On the other hand, it has been recently shown that the use of subject-specific and instant-specific physiological knowledge can improve the accuracy of the clinical feature estimation [7]. Therefore, the GTF approach can benefit significantly from being made adaptive to a variety of physiological state.

This paper presents and experimentally validates a novel adaptive multi-channel (AMC) approach for the reconstruction of the central aortic BP waveform from multiple peripheral BP measurements. The main idea of the AMC algorithm is presented in section II. The experimental methods are covered in section III, and section IV provides the experimental results and discussions.

II. AMC Identification of Arterial Circulation

A. Asymmetric T-Tube Model of Arterial Circulation

The dynamics of the arterial circulatory system can be well described by the "asymmetric T-tube" model [8,9] shown in Fig. 1. The asymmetric T-tube arterial circulatory model is characterized by a parallel connection of 2 distinct transmission lines with the associated load impedances. The transmission lines represent the behavior of the proximal vessels, whereas the load impedances approximate the resultant effect of the distal circulation. The details of the asymmetric T-tube model as well as the nomenclatures in Fig. 1 are well sum-

Jin-Oh Hahn and H. Harry Asada are with d'Arbeloff Laboratory for Information Systems and Technology, Massachusetts Institute of Technology (e-mail: {stardust, asada}@mit.edu).

Andrew Reisner is with Emergency Department, Massachusetts General Hospital (e-mail: areisner@partners.org).

Horacio Hojman is with Department of Surgery, Yale University.

marized in [8,9]. By using the transmission line analogy, the pressure transfer dynamics from the aorta to the peripheries can be expressed as follows, where $P_a(s)$, $P_h(s)$ and $P_b(s)$ are the central aortic, head-end and body-end BP, and γ_h, τ_h, γ_b and τ_b are the head-end and body-end reflection coefficients and time delays associated with the wave transmission, respectively, as shown in Fig. 2:

$$W_h(s) \equiv \frac{P_h(s)}{P_a(s)} = e^{-\tau_h s}\frac{1+\gamma_h}{1+\gamma_h e^{-2\tau_h s}} \equiv e^{-\tau_h s}\Omega_h(s)$$
$$W_b(s) \equiv \frac{P_b(s)}{P_a(s)} = e^{-\tau_b s}\frac{1+\gamma_b}{1+\gamma_b e^{-2\tau_b s}} \equiv e^{-\tau_b s}\Omega_b(s) \quad (1)$$

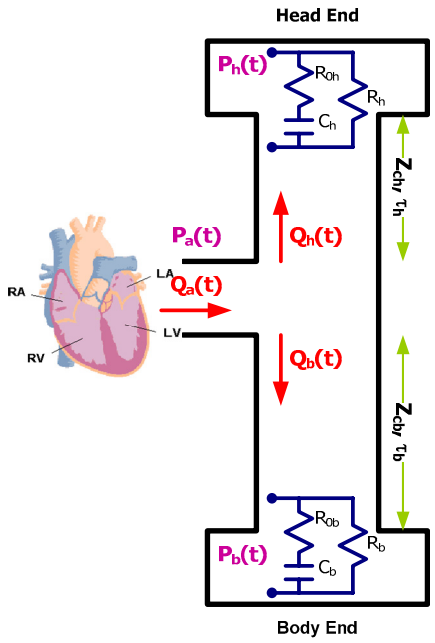

Fig. 1 Asymmetric T-tube model of arterial circulation

Together with the modified Windkessel load impedances as illustrated in Fig. 1, (1) can be rewritten in the following form, where the lumped parameters τ_h, τ_b, β_h, β_b, χ_h and χ_b are physiologic-state-dependent unknowns that are expressed in terms of the physical parameters in Fig. 1 [12]:

$$\Omega_h(s) = \frac{s+\beta_h+\chi_h}{s+\beta_h+\chi_h e^{-2\tau_h s}}$$
$$\Omega_b(s) = e^{-\tau_d s}\frac{s+\beta_b+\chi_b}{s+\beta_b+\chi_b e^{-2\tau_b s}} \quad (2)$$

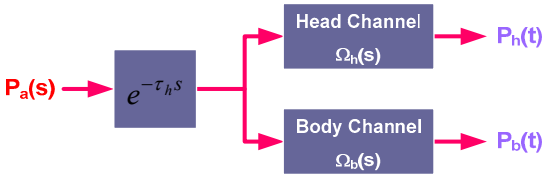

Fig. 2 Pressure transfer dynamics from aorta to peripheries

B. AMC Identification Formulation

In order to avoid the use of the central aortic BP measurement in identifying the pressure transfer dynamics, this paper proposes the application of the multi-channel system identification methodology (which is suited for the identification of systems with multiple output signals but with inaccessible input signal) [10,11] to 2 peripheral BP measurements. Using the 2 AMC set-ups shown in Fig. 3, the problem of the pressure transfer dynamics identification boils down to the problem of identifying the 6 parameters in (2) that satisfy the following channel correlation equations:

$$\Omega_b(s)P_h(s) = \Omega_h(s)P_b(s) \quad (3a)$$

for the forward set-up (a), and

$$\Omega_h^{-1}(s)P_h(s) = \Omega_b^{-1}(s)P_b(s) = P_a(s)e^{-\tau_h s} \quad (3b)$$

for the inverse set-up (b) in Fig. 3, respectively.

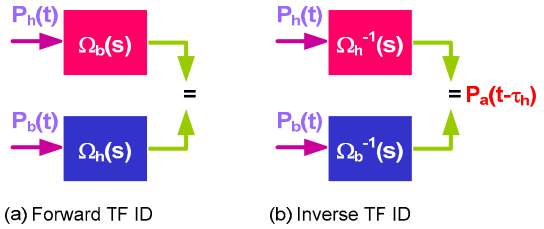

Fig. 3 AMC set-up for T-tube pressure transfer dynamics identification

C. Optimization-Based System Identification

The parameterization for the AMC set-ups in Fig. 3 turns out to be pseudo-linear regressions, whose solutions necessitate the use of nonlinear optimization techniques. The following constrained optimization problem is formulated in order to identify the unknown parameters in (2) and characterize the pressure transfer dynamics [12]:

$$\min\|\Xi\|_2 = \min\|\xi_h(k) - \xi_b(k)\|_2 \quad (4a)$$

with the constraints

$$0 < \tau_h, \tau_b, \beta_h, \beta_b, \chi_h, \chi_b$$
$$0 < \left(1+\lambda_h^{\min}\right)\chi_h < \beta_h < \left(1+\lambda_h^{\max}\right)\chi_h \quad (4b)$$
$$0 < \left(1+\lambda_b^{\min}\right)\chi_b < \beta_b < \left(1+\lambda_b^{\max}\right)\chi_b$$

where

$$\xi_h(s) \equiv \Omega_h^{-1}(s)P_h(s) = \Omega_b^{-1}(s)P_b(s) \equiv \xi_b(s) \quad (4c)$$

Using the identified parameters, the central aortic BP is reconstructed as follows:

$$\hat{P}_a = \frac{1}{2}(\xi_h + \xi_b) \quad (5)$$

III. Methods

A. Experimental Protocol

Under the experimental protocol #01-055 approved by the Massachusetts Institute of Technology Committee on Animal Care, invasive cardiovascular data including the BP waveforms at the foreleg and femoral arteries as well as the aorta were obtained from an anesthetized swine [12]. The foreleg

and femoral BP measurements were then used as the head-end and body-end peripheral BP waveforms, i.e. P_h and P_b in Fig. 1, respectively, to solve the constrained optimization problem defined by (4). Finally, the accuracy of the reconstructed central aortic BP waveform was assessed by comparing it to the BP measurement at the aorta.

TABLE I
Physiological state experienced by the swine: max, min and mean values

HR [bpm]	BP [mmHg]	CO [lpm]	TPR [mmHg/lpm]
172.5 / 85.15	134.79 / 43.04	5.72 / 1.66	34.01 / 18.46
mean: 110.30	mean: 87.90	mean: 3.49	mean: 25.86

B. Clinical Feature Extraction

The AMC algorithm was further applied to the 60 different experimental swine data segments (all of which are 5 seconds in length) in order to assess its performance with respect to a GTF. In order to construct the GTF, 60 head-end pressure transfer dynamics associated with the different experimental data segments were identified by applying a forward system identification procedure to $W_h(s)$ in (1) with the descending aortic BP as input and the foreleg BP as output. Then the arithmetic mean values of each of the identified model parameters were used to define the GTF in this paper.

All the experimental data segments were processed by the AMC algorithm as well as the GTF, and the accuracy of the central aortic BP waveforms synthesized by the AMC algorithm and the GTF were assessed in terms of the ejection duration (the interval between the diastolic minimum and the dicrotic notch) and the systolic BP (the maximum value of BP in every cardiac cycle). The r^2 value (together with the correlation plot) and the 95% limits-of-agreement (together with the Bland-Altman plot) were used as statistical metric to quantify and compare the performance of the AMC and the GTF approaches.

IV. Results And Discussion

The experimental results confirm the efficacy of the AMC algorithm. A representative central aortic BP waveform reconstructed from the experimental swine data is shown in Fig. 4, which clearly indicates that the central aortic BP waveform, especially the gross waveform morphology, can be well reconstructed by the AMC algorithm. Furthermore, the parameter convergence also turned out to be highly consistent over wide-ranging initial conditions.

The clinical promise of the AMC algorithm has been further suggested by its capability to estimate the waveform features of clinical significance, e.g. the ejection duration and the systolic BP, the results of which are shown in Table I, as well as in Fig. 5 and Fig. 6, respectively.

The AMC algorithm turned out to be able to accurately estimate both the ejection duration and the systolic BP, whereas the GTF considered in this paper seems to have relative limitation compared to the AMC algorithm. It is noted, however, that the GTF can also provide estimates for the systolic BP with decent accuracy, which is in accordance with the numerous previous results on the clinical use of the GTF. Considering that the detection of the dicrotic notch (which is a high-frequency characteristic of the central aortic BP waveform) is an essential part of the ejection duration estimation, the limited ejection duration estimation accuracy of the GTF appears to arise from the "averaging" of the high-frequency diversity of the individual pressure transfer dynamics during the derivation of the GTF.

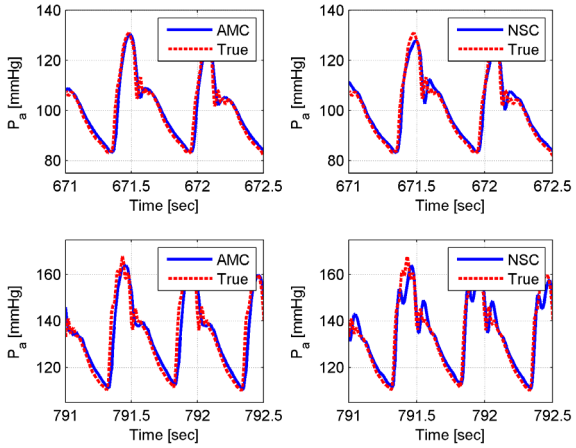

Fig. 4 Results of experiment: The central aortic BP waveform reconstructed by the AMC algorithm is more accurate than its GTF counterpart.

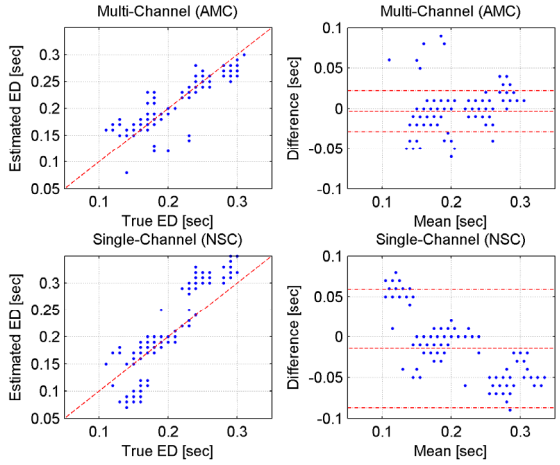

Fig. 5 Ejection duration estimated from reconstructed central blood pressures

It is also possible to interpret the above results in the frequency domain in terms of the frequency responses of the pressure transfer dynamics shown in Fig. 7, which clearly reveals that in contrast to the superb accuracy of the pressure transfer dynamics identified by the AMC algorithm, the GTF suffers from significant disagreement in terms of the location of the peak and the phase response, which in turn yields the mutual contradiction in the accuracy of the time-domain responses in Fig. 4 between the AMC algorithm and the GTF. Indeed, Fig. 4 indicates that while the performance of the

AMC algorithm is highly consistent regardless of the underlying physiological state, the performance of the GTF depends on the underlying physiological state in that it can provide satisfactory central aortic BP waveform when the underlying pressure transfer dynamics is close to the GTF (e.g. at 660 sec), but fails otherwise (e.g. at 780 sec). Hence, the GTF is susceptible to failure if it is conspicuously different from the underlying pressure transfer dynamics of the subject at the specific instant.

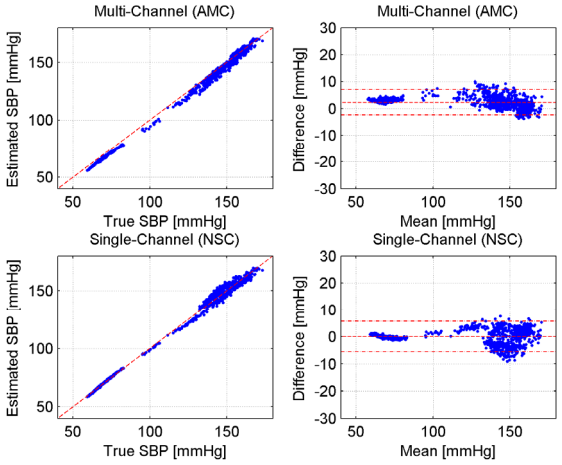

Fig. 6 Systolic BP estimated from reconstructed central blood pressures

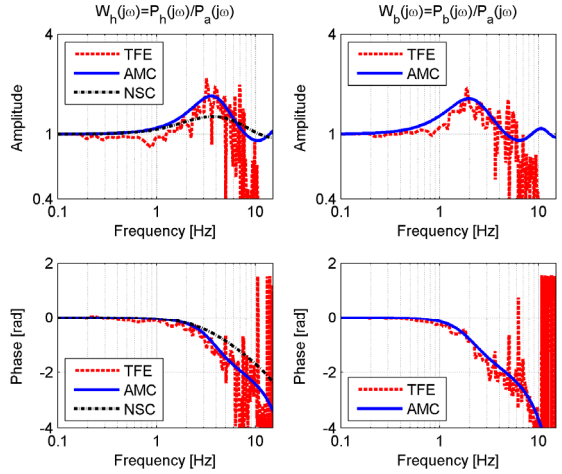

Fig. 7 Frequency responses of true and identified pressure transfer dynamics

The key appeal of the AMC algorithm is that it requires no prior knowledge of the cardiovascular system. Provided with several seconds of the peripheral BP data, it can accurately identify the pressure transfer dynamics and reliably reconstruct the central aortic BP waveform. In this study, the AMC algorithm was superior to one version of GTF in identifying certain clinical features. Moreover, the GTF were first trained to the subject's own data (and would have presumably performed worse if it had been used for other swine subjects). Furthermore, all the GTF alternatives fail to account for subject-specific and state-specific phenomena, and thus their use is controversial [3], [8], [9]. Although the results in this paper cannot be generalized to all swine, let alone humans, it suggests that an adaptive algorithm such as the AMC algorithm might be a more accurate alternative to a GTF (at the expense of necessitating an additional peripheral measurement). Certainly, more extensive investigation on the use of other GTF alternatives as well as the use of larger study population and different species is necessary for a rigorous assessment of the AMC algorithm.

TABLE II
Statistics: BP waveform, ejection duration and systolic BP

	Waveform RMSE	Ejection Duration	Systolic BP
AMC	2.8 ± 1.6 mmHg	-0.004 ± 0.025 sec ($r^2 = 0.9109$)	2.30 ± 4.7 mmHg ($r^2 = 0.9925$)
GTF	3.3 ± 3.5 mmHg	-0.014 ± 0.073 sec ($r^2 = 0.1512$)	0.03 ± 5.6 mmHg ($r^2 = 0.9945$)

ACKNOWLEDGMENT

This material is based upon work supported by the National Science Foundation under Grant No. 0330280.

REFERENCES

[1] B. Fetics, E. Nevo, C.-H. Chen, and D.A. Kass, "Parametric model derivation of transfer function for noninvasive estimation of aortic pressure by radial tonometry," *IEEE Transactions on Biomedical Engineering*, vol. 46, pp. 698-706, 1999.

[2] S.A. Hope, D.B. Tay, I.T. Meredith, and J.D. Cameron, "Use of arterial transfer functions for the derivation of aortic waveform characteristics," *Journal of Hypertension*, vol. 21, pp. 1299-1305, 2003.

[3] P. Segers, S. Carlier, A. Pasquet, S.I. Rabben, L.R. Hellevik, E. Remme, T. De Backer, J. De Sutter, J.D. Thomas, and P. Verdonck, "Individualizing the aorto-radial pressure transfer function: feasibility of a model-based approach," *American Journal of Physiology*, vol. 279, pp. 542-549, 2000.

[4] M. Karamanoglu and M.P. Feneley, "Derivation of the ascending aortic-carotid pressure transfer function with an arterial model," *American Journal of Physiology*, vol. 271, pp. 2399-2404, 1996.

[5] D. Gallagher, A. Adji, and M.F. O'Rourke, "Validation of the transfer function technique for generating central from peripheral upper limb pressure waveform," *American Journal of Hypertension*, vol. 17, pp. 1059-1067, 2004.

[6] S.C. Millasseau, S.J. Patel, S.R. Redwood, J.M. Ritter, and P.J. Chowienczyk, "Pressure wave reflection assessed from the peripheral pulse," *Hypertension*, vol. 41, pp. 1016-1020, 2003.

[7] J.O. Hahn, D.B. McCombie, A.T. Reisner, H.H. Asada, H. Hojman, and R. Mukkamala, "Adaptive left ventricular ejection time estimation using multiple peripheral pressure waveforms," in *Proc. 27th IEEE Engineering in Medicine and Biology Conference*, Shanghai, China, 2005.

[8] K.B. Campbell, R. Burattini, D.L. Bell, R.D. Kirkpatrick, and G.G. Knowlen, "Time-domain formulation of asymmetric T-tube model of arterial system," *American Journal of Physiology*, vol. 258, pp. 1761-1774, 1990.

[9] S.G. Shroff, D.S. Berger, C. Korcarz, R.M. Lang, R.H. Marcus, and D.E. Miller, "Physiological relevance of T-tube model parameters with emphasis on arterial compliance," *American Journal of Physiology*, vol. 269, pp. 365-374, 1995.

[10] M.I. Gurelli and C.L. Nikias, "EVAM: An eigenvector-based algorithm for multichannel blind deconvolution of input colored signals," *IEEE Transactions on Signal Processing*, vol. 43, pp. 134-149, 1995.

[11] G. Xu, H. Liu, L. Tong, and T. Kailath, "A least-squares approach to blind channel identification," *IEEE Transactions on Signal Processing*, vol. 43, pp. 2982-2993, 1995.

[12] J.O. Hahn, A.T. Reisner, and H.H. Asada, "A blind approach to reconstruction of aortic blood pressure waveform using gray-box identification of multiple pressure transfer channels," in *Proc. '2006 American Control Conference*, Minneapolis, USA, 2006.